

**STUDY OF GaN LOW DIMENSIONAL STRUCTURES ON SILICON  
SUBSTRATES GROWN BY THERMAL VAPOR DEPOSITION FOR  
PHOTODIODE AND SOLAR CELL APPLICATIONS**

**By**

**KAMALELDIN MOHAMED ABDALLA ABDELRAHMAN**

**Thesis submitted in fulfillment of the requirements  
for the degree of  
Doctor of Philosophy**

**February 2014**

## DEDICATION

***To my parents:*** Thank you for teaching me to believe in myself while always pushing me to do better. Your advice has helped me to make both the easy and hard decisions and your support has given me the confidence to follow through. I'll need it more than ever in the coming months".

***To my beloved wife and kids:*** Who suffered and sacrificed a lot during my absence from Sudan. Thank you for believing in me; for allowing to me further my studies. Please do not ever doubt my dedication and love you.

***To my brothers:*** Hoping that with this work I have proven to you that there is no mountain higher as long as Allah is on our side. Hoping that you will walk again and be able to fulfil your dreams.

*With respect*

## ACKNOWLEDGMENTS

All praise and thanks to Allah

*All journeys into unknown territory require a knowledgeable guide, and in this journey I have been extremely fortunate to have my supervisor, so I would like to express my sincere appreciation and heartfelt thanks to Professor Md Roslan Hashim. He has provided amazing support and encouragement on a daily basis, a constant stream of ideas (most of which have been extremely useful), vast knowledge, experience, and stimulating discussions. So, really, thanks Professor Roslan.*

*I am also very grateful to Universiti Sains Malaysia for providing financial support for my research and for giving me the chance to be a graduate assistant. I would like to thank all the staff from the School of Physics, Universiti Sains Malaysia, for providing a friendly environment in which I was able to conduct my project smoothly. I would like to thank the technicians of our School, especially the staff in the Nano Optoelectronics Research Laboratory, for their technical support and valuable contribution to my work.*

*Many of the assistant techniques in this thesis were gained through collaborations in our group research and through other friends. I owe a debt of sincere gratitude to the colleagues who assisted me in so many ways for all their valuable support and assistance.*

*Lastly, but by no means least, I would like to express my greatest gratitude to my parents, wife, kids and family for praying for me. I was always able to feel their unconditional love and support, even here, half the world away.*

*K.M. Saron*

## TABLE OF CONTENTS

	Page
<b>DEDICATION</b>	ii
<b>ACKNOWLEDGEMENTS</b>	iii
<b>TABLE OF CONTENTS</b>	iv
<b>LIST OF FIGURES</b>	xi
<b>LIST OF TABLES</b>	xvii
<b>LIST OF SYMBOLS</b>	xix
<b>LIST OF MAJOR ABBREVIATIONS</b>	xxi
<b>ABSTRAK</b>	xxiv
<b>ABSTRACT</b>	xxvi
<b>CHAPTER 1: INTRODUCTION</b>	1
1.1 Introduction	1
1.2 The Problem Statements	5
1.3 Research Objectives	7
1.4 Originality of the Research Work	7
1.5 Outline of the Thesis	8
<b>CHAPTER 2: LITERATURE REVIEW AND THEORETICAL BACKGROUND</b>	9
2.1 Introduction	9
2.2 Background of GaN Growth	9
2.2.1 Overview of GaN Conventional Growth Techniques	11
2.2.1.1 Growth of GaN Low Dimensional Structures and Films using Physical Vapour Deposition (PVD)	12
2.2.1.2 Growth of GaN Low Dimensional Structures and Films by Thermal Chemical Vapour Deposition (TCVD)	13

2.2.2	Overview of GaN Applications	15
2.2.2.1	Overview of GaN-Based Heterojunction Photodiode and Solar Cell	15
2.2.2.2	Overview of GaN-Based UV-Photodetector Metal-Semiconductor-Metal	17
2.3	Thermal Evaporation Process Principles of GaN	18
2.3.1	Synthesis of GaN Low Dimensional Structures	19
2.4	Strain and Stress of the Single-Crystalline GaN	22
2.4.1	Stress Calculation from XRD Data	24
2.4.2	Stress Calculation from Raman Spectra	26
2.5	<i>I-V</i> Characteristics of GaN-Based Junction Diodes	27
2.5.1	Thermionic Emission Method	27
2.5.2	Series Resistance	30
2.5.3	Flat Band Barrier Height ( $\phi_{BF}$ )	30
2.5.4	Temperature Dependent Current-Voltage ( <i>I-V-T</i> ) of GaN/Si Heterostructure	31
2.5.5	Gaussian Modification of Richardson Plots	32
2.5.6	Space Charge Limited-Conduction (SCLC) Mechanism	34
2.6	Fundamental of GaN-Based Devices	35
2.6.1	Fundamentals of p-n Junction	36
2.6.2	The Single-Heterojunction Photodiode	37
2.6.2.1	Responsivity	39
2.6.2.2	Quantum Efficiency	40
2.6.2.3	Response Time	40
2.7	The Photovoltaic Effect	40
2.7.1	Performance of Photovoltage Solar Cell	42
2.7.1.1	Short Circuit Current	43
2.7.1.2	Open Circuit Voltage	43

2.7.1.3	Fill Factor (FF)	43
2.7.1.4	Efficiency	43
2.7.1.5	Resistance	44
2.8	Metal-Semiconductor-Metal (MSM) Photodiode	44
2.8.1	The Schottky Theory of Metal Semiconductor Metal	45
<b>CHAPTER 3: EXPERIMENTAL PROCEDURES</b>		47
3.1	Introduction	47
3.2	NH <sub>3</sub> Free Environment Growth Method of GaN Low Dimensional Structures by PVD	47
3.2.1	Preparing Si Wafers	48
3.2.2	Preparation of Materials	49
3.2.3	Horizontal Tube Furnace Growth Apparatus	49
3.2.4	Growth Conditions of GaN using PVD Technique	51
3.2.4.1	Growth in PVD using Different Carrier Gases	52
3.2.4.2	Growth in PVD using Different Substrate Temperatures	52
3.2.4.3	Growth in PVD at Different Deposition Times	53
3.3	Method of Growing GaN Low Dimensional Structures and Films Using NH <sub>3</sub> Solution by TVD	53
3.3.1	Preparation of Materials	53
3.3.2	Growth Conditions of GaN using NH <sub>3</sub> Solution by TCVD Technique	54
3.3.2.1	Growth of GaN Low Dimensional Structure using Different N <sub>2</sub> Flow Rates	55
3.3.2.2	Growth of GaN Low Dimensional Structure using Different Substrates	55
3.3.2.3	Growth of GaN Films using Different Deposition Time	56
3.4	Metal Contacts Evaporation	56
3.5	<i>I-V</i> Measurement Methods for GaN/Si Heterojunction	57

3.6	Fabrication and Characterization of Devices	58
3.6.1	Fabrication of GaN/Si Heterostructures Photodiode and Solar Cell	58
3.6.2	Characterization of Photodiode Device	60
3.6.3	Characterization of Solar Cell Device	60
3.6.4	Fabrication and Characterization of MSM Photodiode on TCVD Grown GaN Films	60
3.7	Material Characterizations	61
3.7.1	Scanning Electron Microscopy and Energy Dispersive X-Ray	62
3.7.2	X-Ray Diffraction	63
3.7.3	Photoluminescence and Raman Measurements	64
3.7.4	Optical Reflectometer	65
3.7.5	Hall Effect	66
3.7.6	Solar Cell Parameter Measurement System	68
	<b>CHAPTER 4: GROWTH OF GaN LOW DIMENSIONAL STRUCTURES ON Si (111) BY THERMAL VAPOR DEPOSITION IN NH<sub>3</sub>-FREE ENVIRONMENTS</b>	70
4.1	Introduction	70
4.2	Growth of GaN Low Dimensional Structures under Different Carrier Gases	70
4.2.1	Surface Morphology of GaN Low Dimensional Structures	71
4.2.2	XRD Analysis of GaN Low Dimensional Structures	73
4.2.3	Raman Analysis of GaN Structures Grown under Different Carrier Gases	76
4.2.4	Room Temperature Photoluminescence Spectra	78
4.2.5	Current Density–Voltage Characteristics of GaN/Si Junction Diodes	79
4.2.5.1	Current Density-Voltage Characteristics of Heterojunction Diode	80
4.2.6	Temperature Dependent Transport Behaviour of GaN/Si Heterojunction Structure	82

4.2.6.1	Temperature Dependent Current-Voltage Characteristics of GaN/Si Heterojunction Diode	83
4.3	Growth of GaN Low Dimensional Structures at Different Substrate Temperatures	90
4.3.1	Surface Morphology of GaN Low Dimension Structures	91
4.3.2	XRD Analysis of GaN Low Dimensional Structures	94
4.3.3	Raman Spectra of GaN Structures Grown at Different Temperatures	97
4.3.4	Photoluminescence Spectra of Low Dimensional Structures Grown at Different Temperatures	99
4.3.5	Carrier Transport in GaN/n-Si Junction Photodiode (PD) Fabricated at Different Temperatures	101
4.3.5.1	Hall Measurements of GaN Structures Grown on Si at Different Temperatures	102
4.3.5.2	$J-V$ Characteristics of GaN/n-Si Junction Photodiode PVD GaN Structures	104
4.3.5.3	Photodetection of GaN/Si Junctions Prepared at Different Temperatures	106
4.3.6	Solar Cell Measurement of GaN/Si Heterostructure Diodes Fabricated at Different Temperatures	113
4.4	Effect of Deposition Time on Growth of GaN on n-Si (111) Substrate	116
4.4.1	Surface Morphology of GaN Low Dimensional Structures Grown at Different Deposition Times	116
4.4.2	XRD Analysis of GaN Low Dimensional Structures Grown at Different Deposition Time	118
4.4.3	Raman Study of GaN Low Dimensional Structures Grown at Different Deposition Time	119
4.4.4	PL Spectra of GaN Structures Grown at Different Deposition Time	120
4.4.5	Optical Reflection of the as-Grown GaN Films	122
4.4.6	Transport and Photovoltaic Properties of GaN Low Dimension Structures Grown at Different Deposition Time	124
4.5	Summary	129



<b>CHAPTER 5: GROWTH OF GaN LOW DIMENSIONAL STRUCTURES ON Si SUBSTRATES USING NH<sub>3</sub> SOLUTION BY THERMAL VAPOR DEPOSITION</b>	132
5.1 Introduction	132
5.2 Synthesis of GaN Low Dimensional Structures on n-Si (111) by TVD under Controlled N <sub>2</sub> Flow Rate	132
5.2.1 Surface Morphology of GaN Low Dimensional Structures	133
5.2.2 XRD Analysis of GaN Low Dimensional Structures	136
5.2.3 Raman Analysis of GaN Low Dimensional Structures	138
5.2.4 Photoluminescence Spectra of GaN Low Dimensional Structures	140
5.3 Synthesis of GaN Low Dimensional Structures Deposited on Si (111) and Si (100) Substrates by TVD	142
5.3.1 Surface Morphology of GaN Low Dimensional Structures	142
5.3.2 XRD Pattern of GaN Low Dimensional Structures	144
5.3.3 Raman Analysis of GaN Low Dimensional Structures	147
5.3.4 PL Spectra of GaN Low Dimensional Structures	148
5.3.5 Reflection Spectra of GaN Low Dimensional Structures on Si Substrates	149
5.3.6 Electrical Characteristics of GaN/Si Structures	150
5.3.6.1 <i>J-V</i> Characteristics GaN/Si Heterostructure Diodes	151
5.3.6.2 Performance of GaN/Si Heterostructure Photodiodes	155
5.3.6. Performance of GaN/Si Heterostructure Solar Cell	160
5.4 Summary	162
<b>CHAPTER 6: GROWTH OF GaN FILMS ON n-Si (111) USING NH<sub>3</sub> SOLUTION BY THERMAL VAPOR DEPOSITION</b>	164
6.1 Introduction	164
6.2 Growth of GaN Films Using NH <sub>3</sub> Solution by TVD	164
6.2.1 Surface Morphology of GaN Films	164

6.2.2	XRD Analyses of GaN Films	166
6.2.3	Raman Analysis of GaN Films	169
6.2.4	Photoluminescence of GaN Films	170
6.2.5	MSM UV Photodetectors Based on Schottky Barriers of Ni/GaN Films Grown Using $\text{HN}_3$ Solution	172
6.3	Summary	177
	<b>CHAPTER 7: CONCLUSIONS AND FUTURE WORKS</b>	179
	<b>REFERENCES</b>	183
	<b>APPENDICES</b>	205
	<b>Appendix 1: Comparison between the Properties of GaN, Si, AlN and ZnO</b>	205
	<b>LIST OF PUBLICATIONS</b>	206

## LIST OF FIGURES

		Page
Figure 2.1	Quasi-aligned vertical standing GaN NWs under reduced pressure which follows VS transformation [104].	21
Figure 2.2	Schematic for the biaxial stress/strain resulting from the lattice and thermal mismatches between layer and substrates: (a) stress between layer and two different substrates and (b) stress/strain between GaN and Si substrate [114].	24
Figure 2.3	Information from Raman Spectroscopy on the shift in $E_2$ high frequency peak for the hexagonal GaN that provides information about the stress state.	27
Figure 2.4	Schematic energy band alignment diagram of the n-GaN/p-Si heterojunction under thermal equilibrium.	29
Figure 2.5	Schematic representation of the operation of a p-n junction photodiode: (a) geometrical model of the structure and (b) $I$ - $V$ characteristics for the illuminated and non-illuminated photodiode [146].	37
Figure 2.6	Equivalent scheme of a real PV cell under illumination, based on a single-diode model [148].	41
Figure 2.7	A typical $I$ - $V$ curve of a solar cell (Adopted and redrawn from [149]).	42
Figure 2.8	Band gap diagram of the MSM structured photodetector when the bias direction is from M1 to M2 (a) and from M2 to M1 (b).	46
Figure 3.1	Flow chart of GaN grown on Si substrates using TVD.	48
Figure 3.2	(a) Horizontal tube furnace for evaporation of GaN and (b) a schematic diagram of the experimental setup for GaN growth by PVD.	50
Figure 3.3	Schematic diagram of the experimental setup for GaN growth by TCVD using $NH_3$ solution.	54
Figure 3.4	Thermal evaporator chamber and schematic diagram of thermal evaporator.	57
Figure 3.5	Schematic diagram of the $I$ - $V$ measurement process at various temperatures.	58
Figure 3.6	(a) Schematic of the GaN/Si photodiodes and solar cells structure used and (b) measured dark $I$ - $V$ characteristics of	59

	single Ag-Al/GaN and Al/Si measured at RT.	
Figure 3.7	The MSM structure used in the fabrication of UV Schotky diode in this thesis.	61
Figure 3.8	Schematic diagram of the SEM system [156].	62
Figure 3.9	Schematic diagram of a PL system [157].	64
Figure 3.10	A schematic diagram of the Hall effect measurement. There are four contacts at the corners of the sample. The red lines show the Hall voltage across different points with the variation of current and magnetic field polarities.	67
Figure 3.11	Image of the solar simulator and schematic diagram of solar cell $I$ - $V$ measurement system.	69
Figure 4.1	SEM images of GaN low D structures grown on Si (111) using furnace tube under different carrier gases: (a) $N_2$ produced wires and rods; (b) $N_2$ mixed with $H_2$ produced wire and triangles, and (c) Ar produced wires like tree branches and EDX spectra at the right side of SEM images.	72
Figure 4.2	XRD patterns of GaN low D structures grown on n-Si (111) substrate using HTF under different carrier gases: (a) $N_2$ , (b) $N_2$ mixed with $H_2$ , and (c) Ar.	74
Figure 4.3	Raman spectra of GaN low D structures grown using different carrier gases: (a) $N_2$ , (b) $N_2$ mixed with $H_2$ , and (c) Ar. The intense band at $521\text{ cm}^{-1}$ arises from the Si substrate.	77
Figure 4.4	Photoluminescence spectra of GaN low D structures grown with different carrier gases: (a) $N_2$ , (b) $N_2$ mixed $H_2$ , and (c) Ar.	78
Figure 4.5	(a) $J$ - $V$ curve and (b) semi log of $J$ - $V$ , showing the dark $J$ - $V$ characteristics of the GaN low D structures/Si grown under different carrier gases (■) $N_2$ , (▲) $N_2+H_2$ and (○) Ar.	80
Figure 4.6	Temperature dependent $J$ - $V$ semi log plot for GaN/Si heterojunction grown in $N_2$ flow.	83
Figure 4.7	The variations of ideality factor and barrier height as a function of temperature from TE for GaN/Si heterojunction.	85
Figure 4.8	The variation of flat band barrier heights as a function of temperature from TE for GaN/Si heterojunction.	86
Figure 4.9	Conventional Richardson plot, $\ln(J_s/T^2)$ vs. $1/(kT)$ and “modified” Richardson’s plot $\ln J_s/T^2$ vs. $1/nkT$ for the fabricated heterojunction. From the slope of the linear fit of	87

the data, an effective SBH of 1.475 eV was determined.

Figure 4.10	The zero-bias apparent barrier heights extracted from $J$ - $V$ analysis plotted against the $q/2kT$ and ideality factor versus $q/2kT$ according to the Gaussian distribution of the BHs.	88
Figure 4.11	The modified Richardson plots for the extraction of mean SBH $\phi_{B0}$ and mean barrier height of 0.95 eV from $\ln(J_0/T^2) - 0.5\sigma^2 q^2/(kT)^2$ versus $1/kT$ .	89
Figure 4.12	SEM images and EDX spectra of the GaN structures grown on the Si (111) substrate at different temperatures (a) 950, (b) 1000, (c) 1050, and (d) 1100°C.	92
Figure 4.13	XRD patterns of the GaN structures grown on the n-Si (111) substrate at different temperatures (a) 950, (b) 1000, (c) 1050 and (d) 1100°C.	95
Figure 4.14	Raman spectra of the GaN low D structures grown on the Si (111) substrates at different temperatures (a) 950, (b) 1000, (c) 1050 and (d) 1100°C.	98
Figure 4.15	PL emission spectra of GaN structures grown on Si (111) substrate at different temperatures (a) 950°C, (b) 1000°C, (c) 1050°C and (d) 1100°C. The insert shows PL in range from 340 to 440nm.	100
Figure 4.16	Dark $J$ - $V$ versus $V$ plots measured at RT for the GaN/Si diodes grown at different temperatures (a) 950, (b) 1000, (c) 1050 and (d) 1100°C.	104
Figure 4.17	$J$ - $V$ characteristics of three GaN/Si heterojunction PDs measured in dark and under UV 365 nm and visible 15 mW light sources fabricated at different temperatures; (b) 1000, (c) 1050, and (d) 1100°C	106
Figure 4.18	Spectral responsivity of the fabricated GaN low D structures/Si junction PDs at different temperatures (b) 1000, (c) 1050, and (d) 1100°C.	109
Figure 4.19	Measured continuous photoresponse as function of time upon switching of (a) visible light and (b) UV lamp on and off at 2 V bias of GaN/n-Si heterostructure PDs grown at different temperatures (b) 1000, (c) 1050, and (d) 1100°C.	112
Figure 4.20	$J$ - $V$ characteristics of the fabricated GaN/Si solar cells: junctions grown at different temperatures tested under 30 mW/cm <sup>2</sup> illumination and insert is $J$ - $V$ curve of the sample grown at 1100°C.	114
Figure 4.21	SEM images of the GaN low D structures grown on Si (111) after (a) 1h, (b) 2h and (c) 3h. Image (d) is a cross-sectional	117

	view of the film formed after 3h.	
Figure 4.22	XRD patterns of the GaN structured films deposited for (a) 1h, (b) 2h, and (c) 3h.	118
Figure 4.23	Raman spectra of the three GaN films grown for different growth times: (a) 1h, (b) 2h, and (c) 3h.	120
Figure 4.24	The PL emission spectra of GaN structured films grown on Si for (a) 1h, (b) 2h and (c) 3h. The insert is PL emission of as deposited GaN samples in range between 330 and 450 nm.	121
Figure 4.25	Reflection spectra of (a) bare Si (111) and (b) 1 h, (c) 2h and (d) 3h-deposited GaN structures on n-Si (111).	123
Figure 4.26	Room temperature Hall carrier concentration and hole mobility versus deposition time for the GaN structured films.	124
Figure 4.27	<i>J-V</i> characteristics of the GaN/Si junction solar cells deposited at different times; (a) 1h, (b) 2h and (c) 3h tested (a) in dark and (b) under 30 mW/cm <sup>2</sup> illumination.	126
Figure 5.1	SEM images and EDX spectra of the low D structures grown on the Si (111) substrates with NH <sub>3</sub> solution under different N <sub>2</sub> flow rates (a) 1 LPM, (b) 2 LPM, (c) 3 LPM and (d) 4 LPM, and (e) evolution of the structures density as a function of the flow rate.	134
Figure 5.2	XRD patterns of the GaN low D structures grown on the n-Si (111) substrates with aqueous NH <sub>3</sub> under different N <sub>2</sub> flow rates, (a) 1LPM, (b) 2 LPM, (c) 3 LPM, and (d) 4 LPM at 1050°C.	137
Figure 5.3	Raman spectra of GaN low D structures grown on the n-Si (111) substrates with aqueous NH <sub>3</sub> under different N <sub>2</sub> flow rates (a) 1 LPM, (b) 2 LPM, (c) 3 LPM, and (d) 4 LPM at 1050°C	138
Figure 5.4	PL emission spectra of GaN low D structures grown on n-Si (111) with aqueous NH <sub>3</sub> under different N <sub>2</sub> flow rates (a) 1 LPM, (b) 2 LPM, (c) 3 LPM, and (d) 4 LPM. Insert shows the NBE of GaN in PL for range between 340 and 420 nm.	140
Figure 5.5	The SEM images of GaN low D structures grown on three substrates; (a) n-Si (111), (b) p-Si (111), and (c) n-Si (100).	143
Figure 5.6	XRD measurements of GaN low D structures grown on three Si substrates (a) n-Si (111), (b) p-Si (111), and n-Si (100).	145
Figure 5.7	Raman spectra of grown GaN on three different Si substrates; (a) n-Si (111), (b) p-Si (111) and (c) n-Si (100).	147

Figure 5.8	PL spectra of the GaN low D structures grown on three different Si substrates; (a) n-Si (111), (b) p-Si (111), and (c) n-Si (100).The insert is the PL spectra of samples (b) and (c).	149
Figure 5.9	Reflection spectra of a bare n-Si (111) and the as-grown GaN low D structures on n-Si (111) and n-Si (100) substrates	150
Figure 5.10	<i>J-V</i> characteristics of the fabricated GaN/Si junctions measured in dark of GaN low D structures grown on (a) n-Si (111), (b) p-Si (111) and (c) n-Si (100).	152
Figure 5.11	Log-log plots of the <i>J-V</i> characteristic under forward bias for diodes grown on (a) n-Si (111) and (c) n-Si (100).	154
Figure 5.12	The <i>J-V</i> characteristics of the fabricated GaN based photodiodes on (a) n-Si (111) and (c) n-Si (100) substrates measured; in dark (●), under UV light (○) and under visible light (Δ).	156
Figure 5.13	Spectral responsivity of the fabricated GaN structures/Si p–n heterojunction PD at different substrates: (□) n-Si (111) and (●) n-Si (100).	158
Figure 5.14	Measured continuous photoresponse as function of time upon switching of (a) visible light and (b) UV lamp on and off at 2 V bias of GaN based heterostructure PDs grown on n-Si (111) and n-Si (100).	159
Figure 5.15	<i>J-V</i> measurements of the GaN/Si heterojunction solar cells grown on different substrates of n-Si (111) and n-Si (100) under solar simulation of 30 mW/cm <sup>2</sup> .	161
Figure 6.1	EM images, cross-section SEM and EDX spectra of GaN films grown on n-Si (111) for different deposition times (a) 30, (b) 45, (c) 60 min.	165
Figure 6.2	The XRD patterns of the GaN films grown on n-Si (111) for different deposition times (a) 30, (b) 45, and (c) 60 min.	167
Figure 6.3	Raman microscopy spectra of the GaN films grown on n-Si (111) for different deposition times (a) 30, (b) 45, and (c) 60 min.	169
Figure 6.4	PL spectra of the GaN films grown on n-Si (111) for different deposition times (a) 30, (b) 45, and (c) 60 min. Insert shows the UV emission of GaN films in PL for range between 340 and 420 nm.	171
Figure 6.5	<i>I-V</i> characteristics of the fabricated n-GaN films grown at <i>I-V</i> characteristics of the fabricated n-GaN films grown at different deposition times (a) 30, (b) 45 and (c) 60 min as UV MSM photodetectors measured in dark and under UV	174

(365 nm) illumination

- Figure 6.6 Responsivity spectra of Ni/GaN films UV detectors with different deposition times (a) 30, (b) 45, and (c) 60 min. 176
- Figure 6.7 Measured continuous photo response as function of time upon switching of UV lamp on and off at 2V bias of MSM UV PDs on GaN films with different deposition times (a) 30, (b) 45, and (c) 60 min. 177



## LIST OF TABLES

		Page
Table 4.1	The diffraction peak positions of (100) and (002) planes, lattice constants, strain and stress of different samples derived from XRD measurements.	76
Table 4.2	The dark current ( $J_d$ ) measured at +5V, the saturation current, barrier heights, ideality factor, reverse leakage current density (at -2 V) and rectification ratio of different GaN/Si junctions at RT.	82
Table 4.3	The values of BHs and Richardson constant of GaN/Si heterojunction obtained using different methods.	90
Table 4.4	The diffraction angle of (100) and (002) planes, interplanar spacing $d$ , lattice parameters $a$ and $c$ , in plane $\varepsilon_a$ and out plane $\varepsilon_c$ strains and $\sigma_{xx}$ stress.	97
Table 4.5	The $E_2$ -H and A1 (LO) phonon modes detected in the Raman spectra and stress calculated from shift in $E_2$ -H peaks.	99
Table 4.6	The peak positions ( $\lambda$ ) of NBE and YB, peaks intensity (I) of NBE and YB, FWHM, and $I_{NBE}/I_{YB}$ ratio of the GaN structures grown on Si (111) at different temperatures.	100
Table 4.7	Hall measurements of generated p-type doping in the otherwise Si substrate during the growth of GaN on n-Si structures at different substrate temperatures.	103
Table 4.8	Dark $J$ - $V$ characteristics of the fabricated GaN/Si junction PDs at different substrate temperatures.	105
Table 4.9	Photo $J$ - $V$ characteristics of the fabricated GaN/Si junction PDs measured at $\pm 5$ V.	111
Table 4.10	$J$ - $V$ measurements of the GaN/Si (111) solar cells grown at different temperatures.	114
Table 4.11	Solar cell parameters obtained for the GaN/Si heterojunctions deposited at different times.	127
Table 5.1	The peak positions of NBE and YB, peaks intensity of NBE and YB, FWHM, and $I_{NBE}/I_{YB}$ ratio of the GaN low D structures grown on n-Si (111) at different flow rates.	141
Table 5.2	The XRD parameters for GaN nanostructures grown on three different Si substrates.	146

Table 5.3	Photo $J$ - $V$ characteristics of the fabricated GaN/Si PD with $S$ measured at 350 and 650 nm for (a) GaN/n-Si (111) and (c) GaN/n-Si (100).	157
Table 5.4	$J$ - $V$ measurements of the GaN/Si heterojunction solar cells grown on different substrates.	161
Table 6.1	The diffraction peak positions of (100) and (002) planes, interplanar spacing, lattice constants, strain and stress of different thickness ( $t$ ) derived from XRD measurements.	168
Table 6.2	Device measurements at a bias voltage of 5V for dark current ( $I_d$ ), photo current ( $I_{ph}$ ), gain ( $G$ ), responsivity ( $R$ ), quantum efficiency $\eta$ , rise and fall times.	175

## LIST OF SYMBOLS

$\epsilon_o$	Absolute dielectric constant
$T$	Absolute temperature
$\alpha$	Absorption coefficient
$N_A$	Acceptor concentration
$A$	Area
$D$	Average crystal size
$k$	Boltzmann constant
$\mu$	Carrier mobility
$E_C$	Conduction band edge
$\sigma$	Conductivity
$R_c$	Contact resistance
$\beta$	Contrast ratio of photo and dark current
$I$	Current
$J$	Current density
$J$ - $V$	Current density–voltage
$I$ - $V$	Current–voltage
$W_D$	Depletion layer width
$V_d$	Diffusion voltage
$N_D$	Donor concentration
$N_c$	Effective density of states
$p$	Effective dipole moment
$m^*$	Effective mass
$\Delta V$	Electrical polarization
$q$	Electron charge
$m_n$	Electron effective mass
$m_o$	Electron mass
$\mu_n$	Electron mobility
$E_F$	Fermi level of semiconductor
$\phi_{BF}$	Flat band barrier height
$F$	Force
$n$	Free electron concentration
$p$	Free hole concentration
$\nu$	Frequency
$G$	Gain
$R_H$	Hall coefficient
$V_H$	Hall voltage
$m_p$	Hole effective mass
$\mu_p$	Hole mobility
$\theta_i$	Hydrogen atoms coverage at the interface
$n$	Ideality factor
$P_{in}$	Incident solar power

$\theta$	Incident/Diffraction angle
$\infty$	Infinity
$d$	Interplanar spacing of the crystal planes
$a$	Lattice constant along x-axis
$c$	Lattice constant along z-axis
$I_m$	Maximum current
$J_m$	Maximum current density
$P_m$	Maximum output power
$\phi_m$	Metal work function
$(hkl)$	Miller indices
$N_i$	Number of sites (dipole moment) per area at the interface
$\omega$	Photon frequency
$h$	Planck's constant
$\eta$	Quantum efficiency
$\epsilon_r$	Relative dielectric constant
$R$	Resistance
$\rho$	Resistivity
$S$	Responsivity
$A^{**}$	Richardson's constant
$I_o$	Saturation current
$\phi_B$	Schottky barrier height
$E_g$	Semiconductor band gap
$\chi$	Semiconductor electron affinity
$\phi_S$	Semiconductor work function
$R_s$	Series resistance
$I_{SC}$	Short circuit current
$J_{SC}$	Short circuit current density
$R_{sh}$	Shunt resistance
$\sigma_s$	Standard deviation
$\epsilon_a$	Strain along a-axis
$\epsilon_c$	Strain along c-axis
$t$	Thickness
$\tau$	Time
$L_t$	Transfer length
$E_v$	Valence band edge
$V$	Voltage
$\vartheta$	Volume
$\lambda$	Wavelength
$w$	Width
$W_C$	Width of the pad

## LIST OF MAJOR ABBREVIATIONS

Al	Aluminum
NH <sub>3</sub>	Ammonia solution or gas
NH <sub>4</sub> F	Ammonium fluoride
NH <sub>4</sub> OH	Ammonium hydroxide
ARC	Anti-reflection coating
a. u.	Arbitrary unit
Ar <sup>+</sup>	Argon-ion
BE	Band emission
BH	Barrier height
CVD	Chemical vapor deposition
CB	Conduction band
Cu	Copper
c-Si	Crystalline silicon
DI	Deionized water
DC	Direct current
E <sub>2</sub> -H	E <sub>2</sub> (high) phonon mode
EMT	Effective mass theory
e-h	Electron-hole
EDX	Energy dispersive X-ray
Eq	Equation
FF	Fill factor
FWHM	Full width at half maximum
GaN	Gallium nitride
He-Cd	Helium cadmium
HCP	Hexagonal close packed
HMDS	Hexamethyldisilazane
HT	Horizontal tube
HTF	Horizontal tube furnace
HF	Hydrofluoric
InGaN	Indium Gallium nitride
InN	Indium nitride
LPM	Liter per minute

LO	Longitudinal optical
Low D	Low-Dimensional
MIS	Metal insulator semiconductor
MS	Metal semiconductor
MSM	Metal-semiconductor-metal
NBs	Nano belts
NRs	Nano rods
NWs	Nano wires
nm	Nanometer
NBE	Near band edge
Ni	Nickel
PD	Photodiode
PL	Photoluminescence
PV	Photovoltaic
PVD	Physical vapor deposition
KOH	Potassium hydroxide
RCA	Radio Corporation of America
RF	Radio frequency
RT	Room temperature
RMS	Root mean square
rpm	rotation per minute
SEM	Scanning electronic microscopy
SBH	Schottky barrier height
SiO <sub>2</sub>	Silicon dioxide
Ag	Silver
AM0	Solar constant
SCLC	Space charge limited current mechanism
Temp	Temperature
T-I-V	Temperature depend on current voltage characteristics
TCVD	Thermal chemical vapor deposition
TE	Thermal evaporation
TVD	Thermal vapor deposition
TE	Thermionic emission

TED	Transmission electron diffraction
TCO	Transparent conductive oxide
UV	Ultraviolet
VB	Valence band
VT	Vapor transport
VLS	Vapor liquid solid
VS	Vapor-solid
WZ	Wurtzite
XRD	X-ray diffraction
Z-B	Zero-bias
ZB	Zinc blende
ZnO	Zinc oxide

**KAJIAN STRUKTUR GaN BERDIMENSI RENDAH PADA SUBSTRAT  
SILIKON YANG DITUMBUHKAN MENGGUNAKAN PEMENDAPAN WAP  
HABA UNTUK APLIKASI FOTODIOD DAN SEL SURIA**

**ABSTRAK**

Galium nitrida (GaN) merupakan semikonduktor jurang jalur dengan aplikasi dalam peranti elektronik dan optoelektronik kuasa tinggi. Sel suria heterostruktur yang melibatkan struktur GaN berdimensi rendah (D rendah) pada substrak silikon (Si) berhablur tunggal adalah pilihan yang lebih baik kerana ia mempunyai kecekapan kuantum dalaman yang amat berkesan, voltan litar terbuka yang besar, dan kos pemrosesan yang rendah. Tesis ini mengkaji pertumbuhan struktur GaN berdimensi D rendah pada substrat Si menggunakan teknik pemendapan wap haba (TVD) yang murah untuk sel suria dan peranti fotodiod (PD). Pertumbuhan ini dicapai menggunakan dua kaedah. Kaedah pertama melibatkan pertumbuhan struktur GaN D rendah pada n-Si (111) dalam persekitaran bebas  $\text{NH}_3$ , menggunakan TVD melalui penyejatan haba serbuk GaN di bawah pengaruh gas pembawa, suhu substrat dan masa pemendapan yang berbeza. Keputusan menunjukkan bahawa morfologi dan bentuk struktur GaN D rendah amat bergantung pada setiap parameter. Belauan sinar X dan spektrum Raman daripada struktur GaN D rendah menunjukkan bahawa struktur GaN mempunyai struktur wurtzit heksagon. Persekitaran bebas  $\text{NH}_3$  dalam TVD dioptimumkan dengan menggunakan masa pemendapan 1 jam dan suhu pertumbuhan  $1000^\circ\text{C}$  untuk memperoleh struktur D rendah yang seragam dengan kualiti hablur yang baik di samping meningkatkan prestasi PD dan peranti sel suria. Semasa pendedahan pada cahaya tampak dan UV (365nm) sampel yang dioptimum sebagai PD menunjukkan arus yang tinggi diperoleh pada 522.5 di bawah cahaya tampak dan 11.3 di bawah cahaya UV (ultralembayung). Sebagai sel suria,



kecekapan penukaran adalah setinggi 5.78% di bawah 30 pencahayaan  $\text{mW/cm}^2$ . Dalam kaedah yang kedua, pertumbuhan saput dan struktur GaN D rendah dalam TVD menggunakan larutan  $\text{NH}_3$  dijalankan dengan mengubah kadar aliran gas pembawa  $\text{N}_2$  dan satah substrat Si. Sampel yang dioptimumkan (dengan kadar aliran 2 liter/min, (111) satah n-Si) menunjukkan tekanan yang paling rendah dan puncak pemancaran UV tertinggi (363,8 nm) tanpa adanya puncak pemancaran kuning, jika dibandingkan dengan sampel struktur D rendah yang lain. Heterosimpang GaN/n-Si (111) difabrikasikan sebagai PD, yang menunjukkan arus tertinggi 736.8 diperoleh di bawah cahaya tampak dan 5.8 di bawah cahaya UV. Semasa pencahayaan ( $30 \text{ mW/cm}^2$ ), sel suria heterosimpang GaN/n-Si (111) menunjukkan kecekapan penukaran yang lebih tinggi iaitu 6.22%, berbanding dengan 3.69% bagi sel suria GaN/n-Si (100). Akhir sekali, konfigurasi logam-semikonduktor-logam (MSM) berasaskan GaN, iaitu saput pada n-Si (111) difabrikasikan untuk pengesanan UV. Semasa pendedahan pada cahaya UV (365 nm) (UV) pada 5 voltan pincang yang dienap selama 45 minit, pengesan MSM UV menunjukkan kebolehtesponan yang tinggi 0.29 dan kecekapan penukaran 98.3%. Kajian itu menunjukkan kemungkinan mensintesis struktur GaN D rendah diatas substrat pada kos rendah dengan aplikasi yang berpotensi dalam foto pengesanan detection dan fotovoltan sel suria.

# **STUDY OF GaN LOW DIMENSIONAL STRUCTURES ON SILICON SUBSTRATES GROWN BY THERMAL VAPOR DEPOSITION FOR PHOTODIODE AND SOLAR CELL APPLICATIONS**

## **ABSTRACT**

Gallium nitride (GaN) is a greatly promising wide band gap semiconductor with applications in high power electronic and optoelectronic devices. Heterostructure solar cell involving GaN low Dimensional (low D) structures on single crystalline silicon (Si) substrates are the preferable choice as they have excellent internal quantum efficiencies, large open-circuit voltages, and low processing cost. This thesis examines the growth of GaN low D structures on Si substrates using inexpensive thermal vapor deposition (TVD) techniques for solar cell and photodiode (PD) devices. The growth was achieved using two methods. The first method involved the growth of GaN low D structures on n-Si (111) in NH<sub>3</sub>-free environments by TVD via thermal evaporation of GaN powder under different carrier gases, substrate temperatures and deposition times. The result showed that the morphology and shape of GaN low D structures are highly dependent on each parameter. The X-ray diffraction and Raman spectra of the low D structures indicated that the GaN structure had a hexagonal wurtzite structure. The TVD is optimized by using 1h deposition time and 1000°C temperature to obtain uniform dense low D structures with good crystalline quality and hence enhanced performance of PD and solar cell devices. Upon exposure to visible and UV (365nm) lights, the optimized sample work as PD showed high current gain of 522.5 under visible light and current gain of 11.3 under UV light. As solar cell, the conversion efficiency is as high as 5.78% under 30 mW/cm<sup>2</sup> illumination. In the second method, the growth of GaN low D structures and films by TVD using NH<sub>3</sub> solution were

carried out by changing the flow rate of N<sub>2</sub> carrier gas and plane of Si substrates. The optimized sample (with flow rate of 2 liter/min, (111) plane of n-Si) shows the lowest stress and highest UV emission at (363.8 nm) peak with almost no yellow emission peak compared to the other low D structures samples. The GaN/n-Si (111) heterojunction was fabricated as PDs, which showed high current gain of 736.8 under visible light and current gain of 5.8 under UV light. Upon illumination (30 mW/cm<sup>2</sup>), the GaN/n-Si (111) heterojunction solar cell exhibited higher conversion efficiency of 6.22% compared to 3.69% for GaN/n-Si (100) solar cell. Finally, metal-semiconductor-metal (MSM) configurations based on GaN film on n-Si (111) was fabricated for UV detection. Upon exposure to (365 nm) UV light at a 5 bias voltage for the 45 min deposition time, the MSM UV detector exhibited a high responsivity of 0.29 and a conversion efficiency of 98.3%. The study showed the possibility of fabricating GaN low D structures on Si substrates at low-cost with potential applications in photodetection and photovoltaic solar cell.

# CHAPTER 1: INTRODUCTION

## 1.1 Introduction

Over the years, intensive researches on semiconductor materials have been conducted to properly investigate their inherent features and applicability. Wide band gap semiconductor material systems (like SiC, ZnO and III-Nitrides related materials) have been developed and regularly applied in electronics, optoelectronics, and numerous other fields [1-3]. Gallium nitride (GaN) has drawn the most attention for future optoelectronic applications due to its unique properties as a semiconductor material [3]. Their distinct features include high electron mobility, high thermal conductivity, large exciton binding energy (~25meV) at room temperature (RT) and wide and direct bandgap (3.4eV). Other distinct features are high breakdown field, due to relatively stable physical properties even under harsh environments, and better chemical stability. These properties make it suitable for several optoelectronic applications such as; field-emission [4], light-emitting diodes [5], short-wavelength optical devices [3, 6], thermoelectrics [5], sensing [7], and energy conversion photovoltaic solar cell [8, 9]. It is also a suitable material for fabricating photodetectors capable of rejecting near infrared and visible regions of the solar spectrum while retaining near unity quantum efficiency in the UV [9]. Moreover, in optoelectronics, GaN is mainly of interest for its potential as a blue and UV light emitter [3].

Many properties of semiconductor materials are based on their crystalline structure. Two common crystal structures of group III-Nitrides and GaN are the hexagonal close packed (HCP) wurtzite (WZ) and face-centered cubic (FCC) zinc blende (ZB). Wurtzite is the most common crystalline form of GaN due to its

thermodynamic stability in ambient condition, while the ZB is a polymorph derived from WZ at high external pressure. The ZB structure is metastable and may be stabilized by epitaxial growth on Si, GaAs, and SiC under certain growth condition [10, 11]. However, bulk of the research has been centered on the direct-transition bandgap structures of WZ crystal phase, because the growth of the WZ is simpler and less expensive than that of the ZB. In both hexagonal and cubic form, GaN have direct bandgap, indeed, the hexagonal structure is stable and can be grown on various substrates like sapphire, SiC and Si [8]. The most important physical properties of GaN, for both WZ and ZB, significant for electronic devices, are reported and compared with those of Si, AlN and ZnO in the table in Appendix 1 [12, 13].

The past decades has witnessed critical considerations being given to the importance of epitaxial growth in the processing of electronic and optoelectronic devices. Two epitaxial processes are commonly utilized: 1) homo-epitaxy and 2) hetero-epitaxy. Homo-epitaxy involves growth on the substrate of the same material (native substrate) while hetero-epitaxy entails the growth of single crystalline materials on non-native substrates. Hetero-epitaxy is generally used for growing GaN due to lack of homosubstrates. The limitations of GaN-based technology development include; the lack of high quality, large native substrates in large quantities and most of the epitaxial research and device progress depend on heteroepitaxial growth. In the semiconductor technology, most integrated circuits are virtually developed on Si substrates. However, GaN based semiconductor materials have also gained more and more importance in the last two decades. But, Si and conventional III-V materials are not appropriate for fabricating optoelectronic devices in the violet and blue bands of the visible region. Moreover, GaAs based

materials cannot be utilized at soaring temperature. Therefore, GaN is more suited for these areas. GaN based devices are epitaxially grown on Si (111), Al<sub>2</sub>O<sub>3</sub> (0001) (sapphire) or SiC (0001) substrates due to the hexagonal surface symmetry and the lack of suitable and cheap homosubstrates [14-16]. However, growth on these substrates is accompanied by a number of deep-level defects, such as dislocations due to disparity in thermal, lattice mismatch and strain (tensile or compressive), which may control the consistency and applicability of GaN-based devices. As far as Al<sub>2</sub>O<sub>3</sub> is concerned, the low thermal conductivity makes it less suitable for packaging of high power devices. From the lattice constants and thermal coefficient requirements, SiC is the best option although, it is very expensive. A high-quality 4 inch wafer costs about USD3000, whereas wafers of a larger diameter are currently not available [13]. Silicon (Si) has attracted considerable attention as a substrate material for GaN growth because of its high quality, low cost, wide availability in large diameters, accessibility, promising route for large-scale manufacture, and low-cost mass production [13, 17, 18]. These advantages have made GaN growth on Si highly desirable in the Si-based electronic industry. In addition, the integration of well-established Si electronics with GaN-based photonic devices (optoelectronic integrated circuits (OEICs)) has also proved lucrative in the manufacturing industry.

Recently, low dimensional (low D) semiconductor materials have received great attention due to their unique structure, and superior properties. Low D materials are the class of materials whose structural units are nanoscale low D systems such as quantum dots, rods and wires, quantum fractal networks, nanotubes, etc. Because of the quantum confinement effects, the physical properties of such systems are completely different than those of bulk systems. Such materials are becoming firm ground for the improvement of the rapidly developing area, nanotechnology. Due to

the unusual properties of low D functional materials, their potential to be used in energy- and resource-saving technologies is tremendously high. Among the low D structured materials, GaN nanowires are very interesting with the charge carrier confined in a one-dimension (1D) space owing to their special configuration. GaN nanowires represent unique systems for exploring phenomena at the nanoscale and are expected to play a critical role in future electronic and optoelectronic devices.

Most of the device development depends upon epitaxial growth. The properties of GaN-based optoelectronic (OE) devices are influenced by several variables of the fabrication process of GaN. One of the most significant factors is the growth process of GaN low D structures or films, which controls the structural, optical, and electrical properties of GaN epilayers. However, this growth procedure poses a serious problem as a result of the low decomposition of GaN relative to its high melting temperature, the low solubility of nitrogen in Ga and the high equilibrium vapor pressure of nitrogen on GaN at moderate temperatures. Several studies have made efforts to grow GaN with different morphologies, different optical and electrical properties using various growth techniques. These methods include; metal organic chemical vapor deposition (MOCVD) [19, 20], hydride vapour phase epitaxy (HVPE) [21], molecular beam epitaxy (MBE) [22], physical vapor deposition (PVD) via thermal evaporation techniques [23] and chemical vapor deposition (CVD) [8]. Among the widely studied techniques for GaN nanostructures or film growth, the thermal evaporation technique via vapor phase transport has shown the most potential because of its comparatively uncomplicated experimental procedure, its low melting point, low decomposition or low sublimation point oxides, inexpensive method, and high growth GaN yield [24].

## 1.2 The Problem Statements

Several essential problems are addressed in this research, and they are summarized as follows: A major issue for the success of GaN based optoelectronics industry is reducing the device cost and simultaneously integrating the GaN based-device with Si electronics on the same chip. GaN based devices are commonly grown by MBE and MOCVD techniques, both requiring expensive equipment and/or reagents. In the particular case of solar cells applications, it would be essential to find inexpensive preparation techniques of GaN semiconductors. Another important issue in growing GaN is that  $N_2$  molecules have a very strong binding energy, and this makes it becomes impossible to decompose  $N_2$  vapor molecules in the growth chamber by thermal means temperatures. But normally, other precursors as  $NH_3$  gas or atomic nitrogen from a radio frequency source are used to grow GaN low D structures or films. Thermal vapor deposition (TVD) is currently employed to deposit GaN by using a direct reaction of Ga with  $NH_3$  gas. In order to promote the formation of GaN, it is necessary to keep the  $NH_3$  gas partial pressure above 1 bar.

This is even more so that it is practically very difficult to make a fully GaN-based high efficiency solar cell. This is partly related to the relatively inferior quality of GaN crystals grown epitaxially on some heterogeneous substrates, such as SiC and sapphire, as well as to the problems associated with p-type doping in GaN. However, growth of GaN-based device structures on Si is currently achieved by using AlN or  $Si_3N_4$  as buffer layers between the Si and the active layer to reduce defects in the GaN layer. But the insulator properties of  $Si_3N_4$  and AlN have a deleterious effect on transport properties of the junction.



This study, therefore, experimented with a low cost and a conventional TVD method to grow GaN low D structures on Si substrates for photodiodes and solar cells applications. The GaN low D structures were directly grown on Si substrates via the thermal evaporation of two material sources: GaN and Ga in environmental free from  $\text{NH}_3$  and by using  $\text{NH}_3$  solution. Subsequently, the influence of growth parameters on morphology, structure, optical, electrical properties and as well as the heterojunction devices such as photodiodes, solar cell descriptions were also investigated to understand what the growth of GaN low D structures using TVD will produce. This was to investigate whether it will exhibit a facile and inexpensive method to assemble GaN/Si junctions for developing solar cell application materials.

Since the PVD has serious limitations in achieving conformal coverage on high crystalline and optical quality, TCVD has received recent attention as a deposition method for GaN. Hence, if the growth of GaN is performed in  $\text{NH}_3$  solution and the flow rate of  $\text{N}_2$  carrier gas, growth temperatures are controlled, the structure and optical properties of the grown GaN should improve. The fixed volatilization of  $\text{NH}_3$  from solution is expected to have a beneficial effect in promoting formation of GaN. To circumvent the problems associated with p-type doping in GaN, the researcher grew readily attainable GaN structures on n-type Si substrates, so that p-n junction heterostructures are created for photovoltaic characteristics. High temperature growth of GaN low D structures can therefore, significantly, play a role as auto doping, possibly due to the inter-diffusion of the Ga into the Si substrate to produce heavy p-type doped Si surface. The wide-bandgap window layer embedding GaN low D structures can then be used as a simpler solar cell design strategy.

### **1.3 Research Objectives**

The principal objectives of this project can be summarized in the following points:

1. To determine the optimal growth parameters that influence the structural, optical and electrical properties of GaN low dimensional structures grown on n-Si (111) substrates using physical vapor deposition (PVD) technique.
2. To investigate GaN low dimensional structures and films synthesized on Si substrates using thermal chemical vapor deposition (TCVD) techniques under different conditions.
3. To evaluate the performance of GaN/Si heterostructures fabricated using low cost PVD and TCVD as photodiodes and solar cells.

### **1.4 Originality of the Research Work**

The originality of the study is supported by the following points. First, thermal growth of GaN on Si substrates, in  $\text{NH}_3$ -free environments is still active area. This technique could provide a new insight into the use of semiconductor materials with wide band gaps in optoelectronic application. This study demonstrates the excellent potential of GaN low D structures on n-Si substrate for use in heterojunction photovoltaic solar cells. Secondly, the investigation the high unintentional doping levels in the Si substrates through the growth of GaN using high growth temperature. Thirdly, the study employs  $\text{NH}_3$  solution as the nitrogen source for the synthesis of high-quality GaN low dimensional structures using the thermal evaporation method. A review of contemporary studies has shown that the synthesis of GaN low D structures on catalyst-free Si through the vapor reaction of Ga and  $\text{NH}_3$ , using  $\text{NH}_3$  solution as a gas source has not been conducted. The use of  $\text{NH}_3$

solution in thermally grown GaN was found to yield excellent GaN low D structures that exhibit strong photoluminescence properties. Finally, the growth of GaN low D structures using inexpensive method to assemble GaN/Si heterojunction for high performance photodiode that sensing both UV and visible photons was investigated. This achievement, was until now, unreported in current literature.

## **1.5 Outline of the Thesis**

The thesis consists of seven (7) chapters. Chapter 1 provides an overview of the study, from the introduction to originality and objectives of the research. Chapter 2 entails a review of the literature covering growth of GaN and GaN devices, the motivation for the growth of GaN, the principles of thermal evaporation technique and mechanism of GaN growth, the process of growth from the vapor phase, GaN nanostructures formation mechanisms as well as the basic principles of some devices (which have been fabricated in this thesis). Chapter 3 comprehensively describes the methodology and instrumentation used in the study. The results obtained from the research works are analyzed and discussed in Chapters 4, 5 and 6. Chapter 4 elaborates on the properties and applications of the grown GaN low dimensional structures on Si (111) substrate using physical vapor deposition via thermal evaporation of GaN powder under different parameters and conditions. Chapter 5 presents the results of experiments conducted on the thermal vapor deposition of GaN low dimensional structures using  $\text{NH}_3$  solution under different parameters Chapter 6 comprises the experimental results of the synthesis of GaN films via thermal evaporation of Ga and GaN powder using  $\text{NH}_3$  solution and their application as UV photodetectors. Finally, a summary of this study along with suggestions for future works are presented in Chapter 7.

## **CHAPTER 2:**

### **LITERATURE REVIEW AND THEORETICAL BACKGROUND**

#### **2.1 Introduction**

The principles and theories of all subjects involved in this work are presented in this chapter. It begins with a background description and overviews of GaN growth and principles of thermal evaporation method. The review addressed the fundamental principles of thermal evaporation and mechanisms of GaN formation. The fundamental theories of temperature dependence of the current voltage of GaN/Si heterojunction are also addressed. Furthermore, the basic concepts of the devices fabricated in this thesis, which include heterojunction photodiode, solar cell and metal-semiconductor-metal (MSM) photodetector, are briefly described in this chapter.

#### **2.2 Background of GaN Growth**

In the early 1930s, GaN was successfully synthesized as a semiconducting material by passing  $\text{NH}_3$  gas over hot metallic Ga at high temperatures of 700 to 1000°C (Johnson and Crew, 1932) [25]. In 1971, Pankove *et al.*, [26] reported the first device application of GaN, LED with an insulating-to-n-type structure, but the material was still relatively of low quality and inhibited by large surrounding background electron concentration, resulting from native defects usually considered to be nitrogen vacancies. Those studies encountered significant limitations in obtaining high-quality material. The quality of GaN was significantly enhanced in 1983 with the introduction of an AlN buffer layer that helped to nucleate and produce smooth GaN films [27]. Previous works conducted in the 1983s-1995s mainly focused on the growth of p-type GaN [28-32]. Present studies have improved

the growth of GaN by reducing the room temperature (RT) background electron concentration of GaN films and improved p-type GaN has been reported [29]. The successful p-type doping resulted in a great improvement of device performance [30, 31, 33, 34].

The rapid development in the application of GaN in the past 20 years has been made possible by the constant advances in the fabrication and characterization of increasingly smaller structures. The breakthrough in material processes and phenomena at the nanoscale, in addition to further growth of new theoretical and experimental techniques have provided huge chances for the development of original nanostructured materials. The fabrication of low dimensional structure has indeed provided a number of different physical properties such as electronic structure, morphology, quantum tunneling, surface effect, quantum phase transition, quantum size-effect confinement and nonlinear susceptibility enhancements [35-37]. Moreover, the one dimensional (1D) nanostructures such as nanowires (NWs), nanorods (NRs), nanotubes (NTs) and nanobelts (NBs), in the limit of small diameters can exhibit significantly different optical, electrical and magnetic properties from their bulk three-dimension (3D) crystalline structure [36].

During the last ten years, a good number of research communities have been involved into the epitaxial growth of GaN nanostructures with different shapes using various growth techniques [8, 23, 38-40]. Among various nanostructures, nanowires (NWs) are particularly attractive for future nanotechnology applications in the field of electronic and optoelectronic devices. GaN is of particular interest because it has been shown to yield good quality NWs [41] and can be either grown intrinsically n-type or doped p-type by the incorporation of magnesium during growth [42]. The

semiconducting properties of GaN nanostructures are presently being studied for possible utilization in high-power transistors and low-power lighting. The first successful fabrication of GaN NWs was conducted by Han *et al.*, [43]. Ever since, new applications for GaN NWs have been found in field effect transistors and single nanowire light-emitting diodes. Recently, GaN NWs have been used to fabricate UV photodetector (PD) [38], nanolasers (LDs) [39], nanoscale field effect transistors [44], and light-emitting diodes (LEDs) [40]. Although a majority of GaN NWs usage is still experimental, they have the potential to replace carbon nanotubes in numerous electronic and optoelectronic applications.

### **2.2.1 Overview of GaN Conventional Growth Techniques**

Fabrication of high quality electronics devices like LEDs, LDs, PDs and solar cells requires the growth of high quality GaN doped structures. As a result of the lack of native GaN substrates, GaN based nitride semiconductors have been grown hetero-epitaxially on non-native substrates. However, remarkable progress has been made in the growth of high quality epitaxial GaN nanostructures and films by a variety of methods such as; metal organic chemical vapor deposition (MOCVD) [19, 20], hydride vapour phase epitaxy (HVPE) [21], molecular beam epitaxy (MBE) [22], physical vapor deposition (PVD) [23] and chemical vapor deposition (CVD) [8]. MBE entails the growth of very high quality thin films and nanostructures, however, due to the high cost factor and low growth rate, the method is not commercially feasible. Though MOCVD is a commercially viable method for growth of GaN, the inherent use of hazardous gases and high growth temperatures in the process restricts its application, although it is not a problem for optoelectronic devices. In the case of solar cells applications, it would be vital to use cheap fabrication techniques of III-N semiconductors. Physical vapour deposition (PVD)

via the thermal evaporation of solid materials and thermal CVD using a horizontal tube furnace (HTF) are best suited option because of low-cost and simple experimental procedure [8, 23, 45].

The most desirable technique of growing high purity single crystal group III-nitrides would be those in which these nitrides themselves are used as starting material. This has been an objective of many studies. Slack and McNelly [46] proposed a method where high quality AlN powder from the Al metal can be produced using  $AlF_3$  as an intermediate product. The AlN powder can be transformed to a single crystal by sublimation in a closed tungsten crucible or in an open tube with a gas flow. Over the years, physical vapor transport (PVT) has been intensively explored as the technique for the growth of bulk AlN [47]. However, these techniques have been classified as PVD or thermal CVD, based on vapor-phase approach where elevated temperature is usually required. Each method can then be sub-divided into various respective techniques that will be discussed in the following sections.

#### **2.2.1.1 Growth of GaN Low Dimensional Structures and Films using Physical Vapour Deposition (PVD)**

The mechanism of PVD begins when a material is physically released from a source material by heating, and transformed onto a substrate by gas carriers. It explains the solidification of vapour directly onto a surface in a way that no chemical reaction takes place. The most common and important PVD technology for GaN growth is thermal evaporation using a tube furnace. To this point, the best results for the growth of bulk AlN were attained using the PVD method [47]. Several researches have examined the gas composition over heated GaN powder [23, 48-51]. Xiao *et.al.*, [52] studied the thermal stability of GaN by putting GaN powders in

furnace temperatures below 1400°C under a flowing stream of N<sub>2</sub> gas. Stach *et al.*, [53] successfully grew GaN NWs on sapphire substrate via a self-catalytic vapor-liquid-solid (VLS) mechanism at high temperature thermal decomposition of GaN.

Furthermore, Lin *et al.*, [54], fabricated vertically aligned GaN NWs array through the thermal evaporation of GaN powder with the support of HCl gas. Tang *et al.*, [23] fabricated high-quality vertically n-GaN (NWs) on p-cuprous oxide (Cu<sub>2</sub>O) (111) by thermal evaporation of GaN conventional powders without using any catalyst or template. Rodriguez *et al.*, [55] synthesized GaN film by close space vapor transport in vacuum using GaN powder as the source material. Recently, Shekari *et al.*, [24, 56] prepared GaN nanostructures from the vapor phase through the thermal evaporation of GaN powder in high temperature furnace on Si and porous Si substrates. They suggested that the growth condition play a vital part in structural morphology and optical characterization of GaN NWs. Herein, we intend to grow GaN low Dimensional structures on the Si substrates without any catalyst and NH<sub>3</sub> gas via the thermal evaporation of GaN powder using a conventional HTF under different conditions.

#### **2.2.1.2 Growth of GaN Low Dimensional Structures and Films by Thermal Chemical Vapour Deposition (TCVD)**

Thermal chemical vapor deposition (TCVD) or thermal vapor deposition (TVD) is commonly used to manufacture very pure high-performance solid materials [57]. The process is frequently used in the semiconductor industry to produce thin films. The CVD process involves synthesizing the substrate with one or more volatile precursors, which react and/or decompose on the substrate surface to produce the desired deposit. In the TCVD method, the precursor gas is released on the surface of the substrate, where the reaction occurs under thermal conditions. The TCVD



process requires a pressure level of  $10^{-3}$  Torr. Recently, CVD technology has been discovered as a significant application in the fields of science and engineering. It is effective for the preparation of many advanced products, including bulk materials as well as coatings, films, nanostructures and composites. The TCVD technology can also be used for the manufacture of electronics and optoelectronic materials [57]. However, TCVD GaN materials are generally grown by a vapor phase reaction between GaCl or Ga and  $\text{NH}_3$  gas, with  $\text{N}_2$  or  $\text{H}_2$  utilized as the carrier gas [19, 58, 59]. Chang *et al.*, [60] and Zhou *et al.*, [61] demonstrated an example of thermal CVD process through the Au-catalyzed growth of GaN NWs by evaporating Ga or a  $\text{Ga}_2\text{O}_3/\text{Ga}$  mixture under an Ar- $\text{NH}_3$  atmosphere resulting in a morphology of periodic zigzag and diameter-modulated shapes on Si wafers. Recently, studies [8, 62-65] have shown the growth of GaN nanostructures and films by TCVD for electronic application. Nabi *et al.*, [65, 66] synthesized high-quality GaN NWs by pre-treating precursors with aqueous  $\text{NH}_3$ . They found that aqueous  $\text{NH}_3$  effectively enhances the quality GaN NWs.

An evaluation of contemporary studies indicates that the synthesis of GaN nanostructures and films on catalyst-free Si through the vapor reaction of Ga and  $\text{NH}_3$ , with the use of  $\text{NH}_3$  solution as gas source are limited. The use of  $\text{NH}_3$  solution is practical because it's cheap, requires no gas controller, as well as its minimal waste production, and rapid, safe reaction with Ga. The  $\text{NH}_3$  solution is effective on the structural and optical properties of GaN structures. This study involves the synthesis of GaN low D structures and films using simple and low-cost TCVD method directly on Si substrates through the reaction of metallic Ga and  $\text{NH}_3$  solution.

## **2.2.2 Overview of GaN Applications**

Great scientific enthusiasm has been garnered by GaN low dimensional structures because of its possible applications for GaN/Si heterostructures, which could benefit from their distinctive and amenable properties. Some of the various device applications previously reported are discussed in the following.

### **2.2.2.1 Overview of GaN-Based Heterojunction Photodiode and Solar Cell**

In recent times, semiconductor nitrides (III-N) and their ternary alloys have been evaluated as possible options for the fabrication of thin film and tandem solar cells due to their wide range bandgap variation from 0.7 up to 6.2 eV (at 300K), which covers the whole visible range and a large part of the solar spectrum. In addition, they have unique physical, chemical and electric properties and can be obtained as n or p type semiconductors [15, 67]. These features make GaN and related compounds potential materials for the fabrication of p-n junction diode based devices [9, 67, 68]. Nonetheless, advancements in the growth and characteristics of GaN have led to considerable development in device technology. GaN-based photodetectors have been continuously built along with visible-and infrared-range detectors, evolving from Si-based to compound semiconductor based devices such as GaN photodetectors [69]. UV-detecting Schottky diodes using GaN nanostructures were also reported [70]. Photodetectors designed to detect both UV and visible photons are usually based on Si and fabricated using metal Schottky, p-i-n, and p-n structures [69-73]. Therefore, heterojunction diodes involving a wide band gap semiconductor on a single crystalline silicon wafer have a number of prospects such as excellent photoresponse, simple processing steps, and low processing cost compared to that on SiC and Al<sub>2</sub>O<sub>3</sub> [74-76]. Consequently, GaN is considered because of its ability to cover visible short-wavelength and UV light as well as its

high heat tolerance. Both undoped and doped GaN films are being used in solar cell devices [8, 68]. However, the growth of GaN on Si substrates has a number of deep-level defects, such as dislocations as a result of lattice mismatch, and strain (tensile or compressive) which may affect the consistency and performance of GaN-based devices. To avoid this problem, a thin crystalline  $\text{Si}_3\text{N}_4$  or AlN layer was introduced by a nitridation process of the substrate [77-79].

Reichertz *et al.*, [68] reported the growth of p- and n-type GaN dual junction solar cell on a standard n-type Si wafer with a thin AlN buffer layer using MBE. They verified that Al diffusion into the Si substrate during the growth of GaN layers forms a viable silicon solar cell and low series resistance at the GaN/Si heterojunction have been demonstrated [68, 80]. However, the insulating properties of AlN led to a deleterious effect on the transport properties of the junctions. For direct growth of GaN on Si, a thin crystalline  $\text{Si}_3\text{N}_4$  layer formed by a nitridation process of the substrate has been shown beneficial for subsequent deposition of GaN [78]. Some research groups have employed a metallic surfactant layer and some novel buffer techniques [81]. Although these techniques are said to lead to improved epitaxial films, their superiority in photovoltaic applications remains to be demonstrated. Yamaguchi *et al.*, [82] deposited InN and InGaN on p-type Si (111) by plasma assisted (PA) MBE and observed the rectifying behavior of the junctions, whereas Xu *et al.*, [83] studied n-GaN/p-Si junction but observed no rectifying property, probably due to charge accumulation at the interface layers. Recently, many research groups [8, 83, 84] have grown directly GaN on n-Si substrates and showed rectifying property. However, more results are required to clarify this behaviour and therefore will be demonstrated in this work. Several techniques have been reported for operation of GaN low dimensional structures into well-defined

arrays for integrated devices. Lee *et al.*, [85] have fabricated a high-brightness GaN NWs homojunction diode using a dielectrophoresis method. Dislocation free GaN NWs have been grown on Si (111) by MBE and showed the rectifying behavior of the heterostructures [22, 86]. Zhong *et al.*, [87] and Tang *et al.*, [88] have synthesized GaN NRs on n-(111) Si based heterojunction diodes solar cell by CVD. The MOCVD method has been used to grow GaN based heterostructures devices [89, 90]. Tang *et al.*, [8] have conducted controlled synthesis of a vertically aligned p-GaN NRs on n-Si substrate based diodes by thermal evaporation technique.

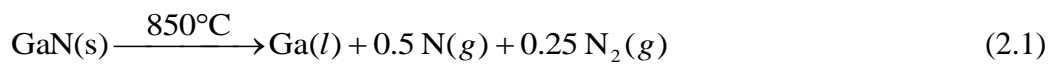
#### **2.2.2.2 Overview of GaN-Based UV-Photodetector Metal-Semiconductor-Metal**

The detection of ultraviolet (UV) radiation is significant for several applications such as environmental, space applications, ozone layer monitoring, flame detection, water purification system, and photochemical phenomena detection, and so on. GaN is one of the most suitable materials for the fabrication of high-responsivity and visible-blind UV detectors, because it has a large direct bandgap energy (3.41eV at RT) and a high saturation electron drift velocity of 310 cm/s [91] as well as high temperature resistance and superior radiation hardness in extreme conditions. In recent times, different types of GaN-based photo devices have been suggested, such as blue, near-UV, and violet light-emitting diodes, laser diodes and metal–semiconductor–metal (MSM) photodetectors [92-98]. Among these devices, MSM photodetector have distinctive features, such as a simple structure, easy fabrication, and readily integration [97, 99]. To acquire exceptional UV photodetector devices based on GaN films with large barrier height, a metal with high work function should be chosen such as nickel (Ni). A simple method for the

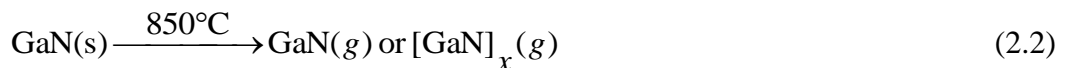
synthesis of GaN films on n-Si (111) substrate based UV photodetector using NH<sub>3</sub> solution is reported here.

### 2.3 Thermal Evaporation Process Principles of GaN

The thermal evaporation method is based on the vapour-solid (V-S) mechanism. Evaporation is a thermal separation process used for concentrating solid into liquid form or (solutions, suspensions, and emulsions). Thermal evaporation technique has been extensively used for growing semiconductor materials in vacuum chamber or in furnace tube. A number of very remarkable nanostructures have been obtained via this method [24, 45, 53, 100]. The conventional TVD growth mechanism remains suitable to account for the growth phenomena of GaN. The growth mechanism can be explained as follows: GaN powder can be thermally evaporated at high temperatures of 1150°C. The decomposition of the GaN nanoparticles generates N atoms and isolated nanoscale Ga droplet. Lvov [48] suggested that GaN decomposes at temperatures above 850°C in high vacuum via the following possible reactions:



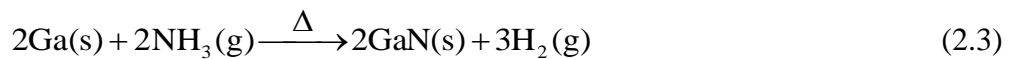
It has also been suggested and experimentally shown that congruent sublimation of GaN is likely, which yields diatomic or polymeric vapor species [48, 101].



Initially, decomposition of the GaN powder leads to the formation of isolated liquid Ga nanoparticles. The resultant vapor species is composed of the atomic nitrogen and diatomic or polymeric GaN. The occurrence of this decomposition in the course of

the thermal evaporation of GaN powder in a furnace tube at 1150°C can be observed to result in low D structures growth in real time and at high spatial resolution [45]. Therefore, it can be deduced that Ga droplets become self-catalytic growth elements of GaN via V-S growth mechanism. Many factors can influence the decomposition and growth of GaN via thermal evaporation of GaN powder such as gas flow rate, type of carrier gas, growth temperatures and growth time.

The second method involves the growth of GaN low D structures and films via the thermal evaporation of Ga under NH<sub>3</sub> gas flow. The growth of GaN in a HTF through the reaction of metallic Ga and NH<sub>3</sub> solution as source materials and N<sub>2</sub> as carrier gas is clarified by the following process: N<sub>2</sub> gas carries volatile NH<sub>3</sub> from the solution into the HTF, then as the temperature of the furnace reached growth temperature (T>950°C), Ga vapor subsequently reacts with gaseous NH<sub>3</sub> to form the nucleus of the GaN. GaN low D structures prepared by a direct reaction of Ga and NH<sub>3</sub> gas in the furnace tube at temperature above 950°C can be expressed by [102];



The gaseous NH<sub>3</sub> flow can be managed by fluctuating the rate by which (N<sub>2</sub> or Ar) gas carries volatile NH<sub>3</sub> from the NH<sub>3</sub> solution into the HTF. In thermal CVD processes, the surface reaction rate on the substrate increases with temperature. Therefore, shape, morphology, and density of nanostructures can be controlled by varying the growth condition such as gas flow rate, growth duration *etc.* [45].

### 2.3.1 Synthesis of GaN Low Dimensional Structures

Several synthetic methods have been developed to successfully fabricate high crystalline quality low D structures for a number of diverse materials ranging from

metals and semiconductors to oxides. For the PVD process, only the vapor-solid growth mechanisms can occur while both vapour-liquid-solid (V-L-S) and V-S growth mechanisms can occur in CVD process. For V-L-S method, catalyst seeds are needed. During the reaction, the catalyst seeds are in liquid form, and the droplets provide preferential sites for absorption of the gas phase reactant. Factors such as deposition time, temperature and carrier gas flow are vital for the growth mechanism that controls the final structural features of GaN nanostructures. GaN nanostructures fabricated explicitly for applications in electronic and optoelectronic nanodevices are typically synthesized using thermal evaporation, a form of self-growth mode control [23]. For nanomaterial fabrication using CVD, reactants are transported from a liquid or gas source to the substrate surface, which absorbs the reactants. The self-induced approach is a valuable growth mode to form GaN nanowires on a wide number of substrates for optoelectronic devices. However, their nucleation and growth processes should be distinguished from the usual growth modes in chemical and physical vapor deposition.

The self-induced growth of GaN in low D structures is more promising than common catalyst-induced growth, since such an approach has the significant advantage to limit the potential nanostructures contamination. Thus, there are increasing efforts to grow low dimensional structures by catalyst-free methods, but in this case a model forecasting the low dimensional structures (NW, NR, etc.) properties is lacking. We synthesized GaN low dimensional structures in the catalyst-free approach on Si substrates via V-S mechanism. Various hierarchical semiconductor nanostructures through the V-S growth mode have also been reported [23, 42, 54]. It must be mentioned here that nanostructures size can be varied by changing the evaporation conditions but no precise control of spatial arrangement

can be achieved. The thermal evaporation basically follows the V-S mechanism. Usually GaN powders are placed inside a HTF, and then GaN powder will be heated up by a heating source to its vapour point once the appropriate pressure within the furnace tube is reached. The vaporized GaN will condense along the surfaces of substrates through the vapour-solid mechanism. The kinetics of this growth process has been reported [103, 104]. As apparent from Figure 2.1, the self-catalytic growth involves two different steps, mainly nucleation and growth. For low pressure, GaN nucleation is free from catalysts and the growth is expected to be via the V-S route.

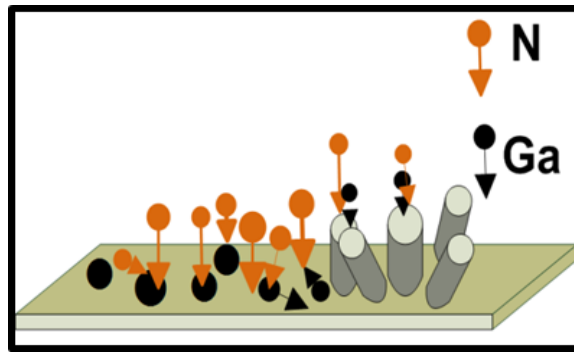


Figure 2.1. Quasi-aligned vertical standing GaN NWs under reduced pressure which follows V-S transformation [104].

Low D structures can be grown without extra metal catalysts by thermally evaporating a suitable source material near its melting point and then depositing at cooler temperatures [105]. The growth of GaN low D structures on a Si substrate by the supply of sufficient metal Ga under atmospheric pressure in TVD system can be explained in the following way. Initially, the Ga vapor can be transported to the substrate at high temperatures which forms liquid droplets with a small size. The supply of  $\text{NH}_3$  and carrier gas contributes to the Ga rich GaN nucleation. The adatoms diffusion of nitrogen radicals in the Ga liquid droplet is expected to be high under atmospheric pressure, favoring crystallization at the substrate–liquid interface



and then growth proceeds by a continuous supply of Ga and  $\text{NH}_3$  that keeps the liquid droplets alive on the tip of the structures. In the case of self-catalytic GaN low D wires, the Ga metal droplet is normally not observed on the apex as the growth proceeds at a higher temperature and results in consumption or desorption of Ga [103]. When  $\text{NH}_3$  is added to the reaction tube furnace, the liquid droplets solidify quickly by nitrogen and the formation of GaN low D wires can eventually be observed [105].

The substrate plane and crystalline structure also affect the growth process. Since Si has a diamond structure, there are two commonly used faces of Si substrates with directions of (111) and (100). Several groups have reported high quality GaN epitaxy directly on Si (111) and Si (100) substrates [63, 106]. GaN grown on Si (100) usually has mixed phases due to the large lattice mismatch and the formation of an amorphous  $\text{Si}_x\text{N}_y$  layer at the interface of GaN/Si, which degrades the crystal quality [107]. However, growth of GaN on Si (100) is very challenging due to the different crystallographic surface symmetries: GaN has six-fold symmetry, while Si (100) has four-fold symmetry [106]. The Si (111) substrate is usually preferred for GaN epitaxy due to the six-fold surface symmetry, which already gives a good rotational matching for GaN [106]. Therefore, good crystalline quality GaN structures have been obtained on Si (111) substrate [88, 108].

#### **2.4 Strain and Stress of the Single Crystalline GaN**

It is acknowledged that epitaxial GaN films or nanostructures with high crystalline quality are required in many optoelectronic applications [8, 9, 88]. However, the epitaxial GaN films have been fabricated on Si (111),  $\text{Al}_2\text{O}_3$  (0001) (sapphire) or SiC (0001) substrates due to the hexagonal surface symmetry [109,

110]. These substrates exhibit different thermal and lattice mismatch compared to GaN, which result in tensile or compressive strain subsequently resulting in the formation of defects such as misfit dislocations. Drawbacks of Si substrates include large mismatches in lattice constants (17%) and thermal expansion coefficients (33%), which lead to strain in the grown layer thereby resulting in the formation of cracks [13, 18, 99, 109, 111]. The thermal expansion coefficient for the silicon substrate is  $\alpha_{\text{Si}}=2.6\times 10^{-6} \text{ K}^{-1}$ , which is smaller than that ( $\alpha_{\text{GaN}}=2.6\times 10^{-6} \text{ K}^{-1}$ ) of GaN. The huge mismatch in thermal expansion coefficients can cause thermal tensile stress and result in severe cracking of the GaN layer during the post-growth cooling process [112]. This problem can be prevented by alternating layers in order to withstand the strain and produce high-quality crystal [110, 111]. In GaN epilayer on Si, stress develops largely from lattice and thermal mismatch between the film and the substrate and growth process [110]. The calculated stresses and the interfacial energy corresponded to the case where the misfit between the GaN layer and the substrate lattice constants is fully relaxed or partially by an array of evenly-spaced edge dislocations. Such a situation is shown schematically in Figure 2. 2 (a). For a partially relaxed layer two cases are possible:

- (1)  $a_{\text{epi}} < a_s$  the layer is under tensile stress
- (2)  $a_{\text{epi}} > a_s$  the layer is under compressive stress

where  $a_{\text{epi}}$  is the lattice constant of epitaxial layer and  $a_s$  lattice constant of substrate. For GaN/Si the lattice constant ( $a_{\text{epi}}=3.189 \text{ \AA}$ ) of GaN layer is smaller than c-Si ( $a_{\text{Si}} = 5.4309 \text{ \AA}$ ), which indicate that the GaN layer under tensile strain (Figure 2. 2 (b)) [113, 114]. The growth on such a substrate allows us to investigate the impact of strain on the optical properties within a single substrate. The stress in GaN can be

estimated from the X-ray diffraction peak positions of GaN planes, and from the Raman scattering peak.

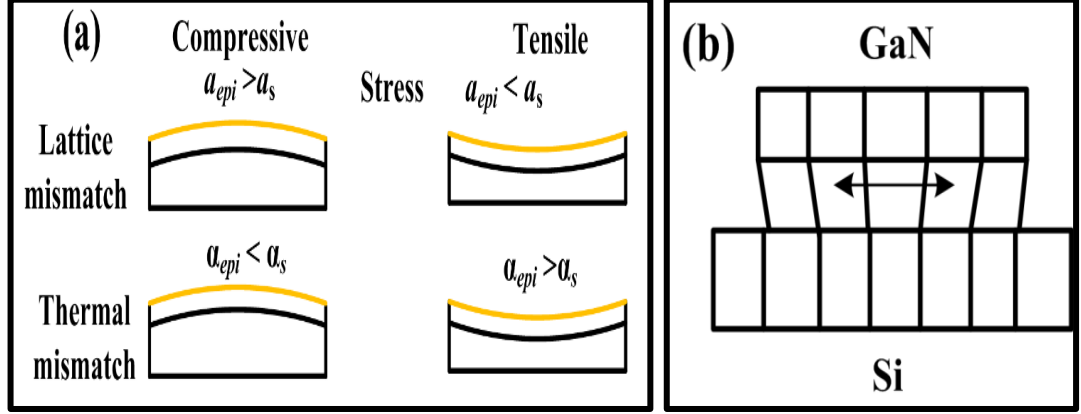


Figure 2.2. Schematic for the biaxial stress/strain resulting from the lattice and thermal mismatches between layer and substrates: (a) stress between layer and two different substrates and (b) stress/strain between GaN and Si substrate [114].

#### 2.4.1 Stress Calculation from XRD Data

Stress and lattice constants are important aspects considered in evaluating the deformation state of crystalline materials. Therefore, the lattice constants,  $c$  and  $a$ , obtained from the XRD measurements can be derived from the peak positions of (100) and (002) planes [115, 116]. The ratio of elastic stiffness constants for epilayer can be inferred from experimental XRD data of GaN epitaxial layer, lattice constants  $c_{epi}$  and  $a_{epi}$ . These are compared with the lattice constants  $a_0$  and  $c_0$  of bulk GaN at 3.189 and 5.185 Å, respectively. Using these values, the in-plane, ( $\epsilon_a$ ), and out-of-plane, ( $\epsilon_c$ ), strain components of the GaN layer can be calculated based on the following expressions [110, 117];

$$\epsilon_a = \frac{(a_{epi} - a_0)}{a_0} \quad (2.4)$$